Bull. Astr. Soc. India (1997) **25**, 217–225

Geometrical and physical description of the two-body problem in Maneff's gravitational field

Cristina Stoica

Institute for Gravitation and Space Sciences, Laboratory for Gravitation, Bd. Ana Ipatescu 21, 71111 Bucharest, Romania

Vasile Mioc

Astronomical Institute of the Romanian Academy, Astronomical Observatory, Str. Ciresilor 19, 3400 Cluj-Napoca, Romania

Received 25 March 1996; accepted 4 July 1996

Abstract. A qualitative study of the two-body problem in Maneff's gravitational field is being performed by representing the motion in the (1/r, $\dot{r}$-plane. The phase trajectories are found to be only conic sections (or arcs of them). Each allowed trajectory is interpreted from the standpoint of physical motion. Concrete astronomical exemplifications are made.

Key words : celestial mechanics - Maneff's field - two-body problem - qualitative theory

1. Introduction

The general relativity theory succeeded in answering many important questions in physics and astronomy; in particular it showed that the natural, unperturbed motion in the solar system is precessional (the trajectories are conic sections whose focal axes rotate in the plane of motion). Unfortunately, as regards the usefulness of such a tool for celestial mechanics, all attempts to formulate a meaningful relativistic n-body problem have failed to provide valuable results (Diacu *et al.* 1995). A gravitational model able to offer to astronomy the same answers as the relativity and equally respond to the theoretical needs of celestial mechanics was therefore necessary.

Such a model is that proposed by Maneff (1924, 1925, 1930a, b) on the basis of physical principles. Unlike other nonrelativistic laws, which generally fail (from an applicative astronomical standpoint) in explaining simultaneously the perihelion advance of inner planets

and the Moon's perigee motion, this law describes accurately both these issues. Fallen into oblivion for half a century, then pointed out by Hagihara (1975) as providing - at least at the solar system level - an equally good justification as the relativity, and finally reconsidered by Daicu (1993), Maneff's field appeared much less commonplace and much more unusual than at first sight. To quote some recent results within this framework, Diacu (1996) proved that Maneff's case represents the only bifurcation of the flow among all quasihomogeneous potentials. For the two-body problem, the analytic solution and the local flow near collision - pointing out the *black hole effect* (spiral collisions) and the nonregularizability of collisions with respect to the initial data - were obtained by Diacu *et al.* (1995), while Mioc & Stoica (1995a, b) gave the general solution of the regularized equations. The isosceles three-body case was tackled by Diacu (1993).

Let us compare Maneff's model with Newton's one from the astronomical point of view, as regards the solar system. The classical standpoint is that the orbit of an object around the Sun must be an ellipse/parabola/hyperbola (depending on the initial conditions). But the perturbations of the other objects in the system (modelled by a many-body problem) make the orbit actually to be a *precessional* ellipse/parabola/hyperbola (or even a more complicated curve). Unfortunately, within this classical framework, the theoretical calculations do not fit the observations, especially for those objects which come close to the Sun; the perihelion advance of Mercury and of the other inner planets cannot be fully explained by Newton's model.

The study of motions in the solar system (and not only) can be maintained within the framework of classical mechanics if one resorts to Maneff's model, and this is particularly convenient for celestial mechanics (Delgado *et al.* 1996). Moreover, using the KAM theory, Lacomba *et al.* (1991) proved that if the motion equations corresponding to Maneff's law are slightly perturbed by some outer force, not necessarily Hamiltonian, most invariant cylinders and tori are topologically preserved under this perturbation. This physically means that the unperturbed orbit of a celestial object around the Sun is a precessional conic section, the apsidal motion becoming more evident the closer the orbit is to the Sun. Under the perturbations of the other bodies, the orbit continues to remain, in general, a precessional conic section. (There are, of course, exceptions, but they are unlikely, because the set of initial data leading to them has measure zero.)

In this paper we perform a qualitative analysis of the two-body problem in Maneff's field, based on the geometrical representation of the motion in the $(1/r, \dot{r})$-plane, where the corresponding phase trajectories are found to be only conic sections (nondegenerate or degenerate) or arcs of them. Each allowed trajectory is interpreted in terms of physical motion, obtaining in this way a wide geometrical and physical picture of the problem. The results are then considered from the astronomical viewpoint, using concrete astrophysical situations.

2. Equations of motion and first integrals

Consider two particles of masses m_1 and m_2, separated by the distance r, which interact according to Maneff's law featured by the potential function (see e.g. Daicu 1993)

$$U = (Gm_1m_2/r)[1 + 3G(m_1 + m_2)/(2c^2r)], \tag{1}$$

where G stands for the Newtonian gravitational constant, while c is the speed of light. It is easy to see that, reducing the problem to a central force problem, the relative motion of m_2, say, with respect to m_1 is planar and described by the following equations in polar coordinates (r, u):

$$\ddot{r} - r\dot{u}^2 = -\mu/r^2 - 3(\mu/c)^2/r^3, \tag{2}$$

$$r\ddot{u} + 2\dot{r}\dot{u} = 0, \tag{3}$$

where $\mu = G(m_1 + m_2)$ and dots mark time-differentiation.

The force field being central, the angular momentum is conserved, and (3) provides the first integral

$$r^2\dot{u} = C, \tag{4}$$

with C = constant angular momentum. The first integral of energy can also be easily obtained, by the usual technique, as

$$\dot{r}^2 + r^2\dot{u}^2 - 2\mu/r - 3(\mu/c)^2 = h, \tag{5}$$

where h = constant of energy. The constants C and h are fully determined by the initial conditions $(r, u, \dot{r}, \dot{u})(t_0) = (r_0, u_0, \dot{r}_0, \dot{u}_0)$.

The analytic solution of the problem can be obtained in closed form. For instance, in the case of nonradial motion ($C \neq 0$), (2) and (4) lead to the Binet-type equation

$$d^2(1/r)/du^2 + [1 - 3(\mu/c)^2/C^2](1/r) = \mu/C^2, \tag{6}$$

with the initial data $(1/r, d(1/r)/du)(u_0) = (1/r_0, -\dot{r}_0/C)$. According to the values of the parameter $[1 - 3(\mu/c)^2/C^2]$, the general solution of the initial value problem attached to equation (6) will be for (a) $C^2 < 3(\mu/c)^2$; (b) $C^2 = 3(\mu/c)^2$; (c) $C^2 > 3(\mu/c)^2$, respectively:

$$r(u) = \left[\left(\frac{1}{r_0} + \frac{\mu}{3(\mu/c)^2 - C^2}\right)\tilde{C}_u - \frac{\dot{r}_0}{\sqrt{3(\mu/c)^2 - C^2}}\tilde{S}_u - \frac{\mu}{3(\mu/c)^2 - C^2}\right]^{-1}; \tag{7a}$$

$$r(u) = \left[\frac{\mu}{2C^2}(u - u_0)^2 - \frac{\dot{r}_0}{C}(u - u_0) + \frac{1}{r_0}\right]^{-1}; \tag{7b}$$

$$r(u) = \left[\left(\frac{1}{r_0} - \frac{\mu}{C^2 - 3(\mu/c)^2}\right)C_u - \frac{\dot{r}_0}{\sqrt{C^2 - 3(\mu/c)^2}}S_u + \frac{\mu}{C^2 - 3(\mu/c)^2}\right]^{-1}, \tag{7c}$$

where we abridged

$$(\tilde{S}_u\ ,\ \tilde{C}_u) = (\sinh, \cosh)\left[\sqrt{3(\mu/c)^2 - / C^2 - 1}\ (u - u_0)\right],$$

$$(S_u, C_u) = (\sin, \cos)\left[\sqrt{1 - 3(\mu/c)^2 / C^2}\ (u - u_0)\right].$$

Equivalent formulae were obtained by Diacu *et al.* (1995) and Delgado *et al.* (1996), who showed that these solutions can be interpreted as representing precessional conic sections.

The radial case (C = 0) can also be solved, by resorting to (5) with $\dot{u} = 0$. But, on the one hand, the analytic solution of the respective equation will be of the form t = t(r), relation invertible only in particular cases; on the other hand, we are more interested in the geometrical and physical global properties of the motion. Anyway, the analysis we are going to perform in the next sections covers both cases.

3. Geometrical description

To study the motion from a qualitative standpoint, we eliminate $\dot{u}$ between (4) and (5), obtaining

$$[C^2 - 3(\mu/c)^2]/r^2 - 2\mu / r + \dot{r}^2 - h = 0. \tag{8}$$

This represents in the (1/r, $\dot{r}$) - plane a family of conic sections whose kind (ellipses, parabolas, hyperbolas) and nature (nondegenerate, degenerate) are respectively given by the parameters

$$\delta = C^2 - 3(\mu/c)^2, \tag{9}$$

$$\Delta = h[3(\mu/c)^2 - C^2] - \mu^2 = -(h\delta + \mu^2). \tag{10}$$

Observe that there exists a critical energy level

$$h_c = -\mu^2/\delta, \tag{11}$$

for which $\Delta = 0$ (degenerate conic sections).

Let $C^2 < 3(\mu/c)^2$; this means $\delta < 0$ and $h_c > 0$. If $h < h_c$, (8) represents a family of hyperbolas (figure 1), centered in $(\mu/\delta, 0)$, of semiaxes $\sqrt{(h - h_c)/\delta}$ and $\sqrt{h_c - h}$, and with foci lying on the (1/r) - axis. For $h = h_c$, (8) represents the corresponding asymptotes, and the family of conjugate hyperbolas for $h > h_c$.

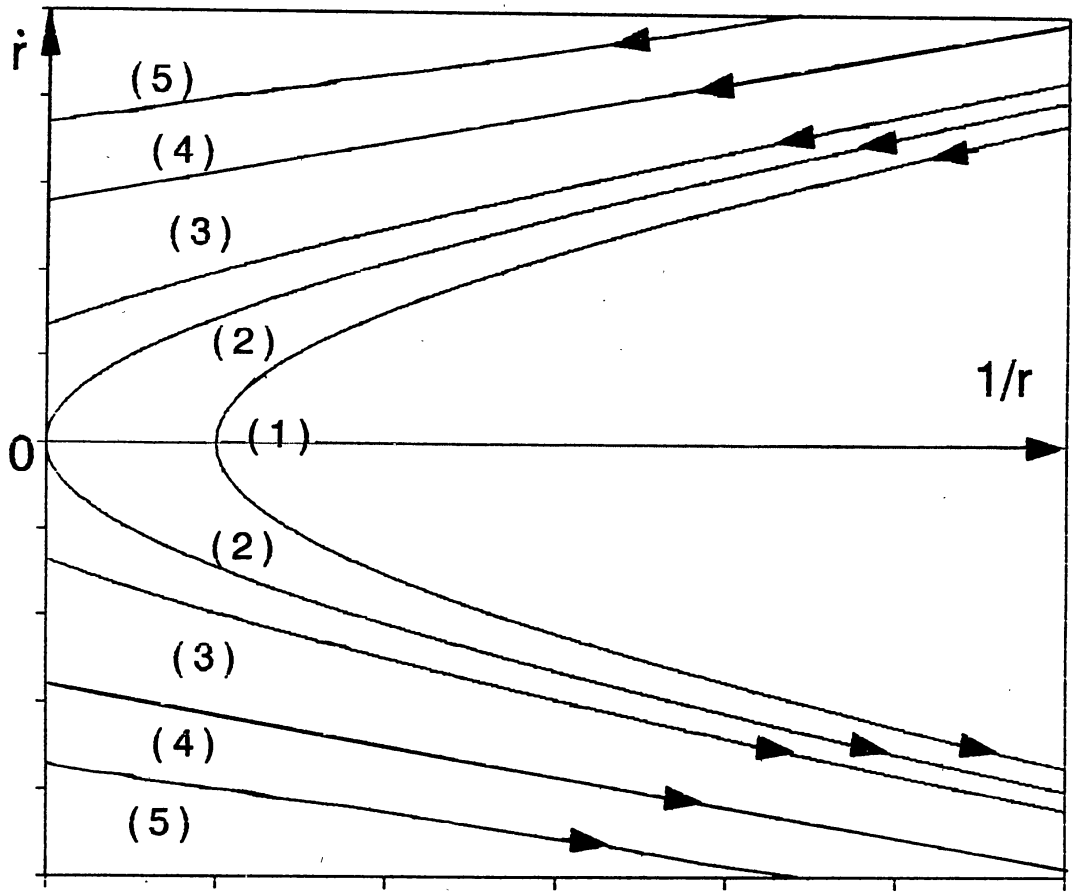

Figure 1. Phase portrait for $\delta < 0$ and : $h < 0$ (1); $h = 0$ (2); $0 < h < h_c$ (3); $h = h_c$ (4); $h > h_c$ (5)

If $C^2 = 3(\mu/c)^2$, this implies $\delta = 0$, and (8) represents a family of (nondegenerate) parabolas with foci lying on the (1/r)-axis (figure 2).

If $C^2 > 3(\mu/c)^2$, we have $\delta > 0$ and $h_c < 0$. Equation (8) represents a family of ellipses with foci lying on the (1/r)-axis (figure 3), and with the same centre and semiaxes as the above hyperbolas. The ellipses are real for $h > h_c$ ($\Delta < 0$), degenerate into the centre of the family if $h = h_c$, and are imaginary (impossible real motion) for $h < h_c$.

Observe that figures 1-3 plot only the curves lying in the halfplane $1/r > 0$ (only these ones represent real motion in the physical plane). That is why in figure 1 the phase trajectories can be: one branch of hyperbola for $h \leq 0$ (tangent to the ṙ-axis if $h = 0$); arcs of one branch of hyperbola for $0 < h < h_c$; portions of the asymptotes for $h = h_c$; arcs of two branches of hyperbola for $h > h_c$. For the same reason, the phase curves in figures 2 and 3 are parabolas/ellipses fully contained in the allowed halfplane for $h \leq 0$ (tangent to the ṙ-axis if $h = 0$), and arcs of such conic sections for $h > 0$.

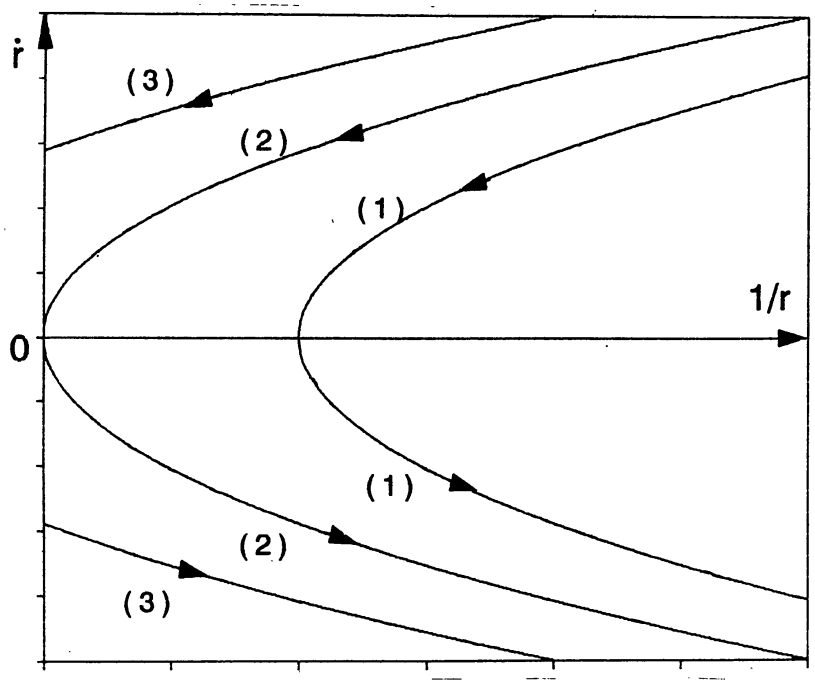

Figure 2. Phase portrait for $\delta = 0$ and : $h < 0$ (1); $h = 0$ (2); $h > 0$ (3).

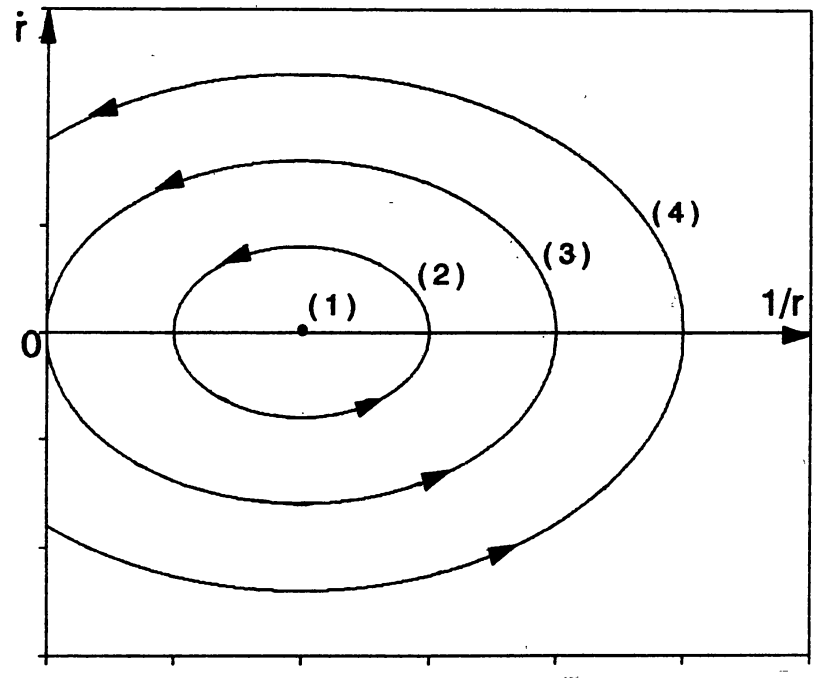

Figure 3. Phase portrait for $\delta > 0$ and : $h = h_c$ (1); $h_c < h < 0$ (2); $h = 0$ (3); $h > 0$ (4)

The use of the (1/r, ṙ)-plane to the geometrical description of the problem has a great advantage: the trajectories are conic sections, whose behaviour is very well known (and this fact facilitates the physical interpretation), while the usual (r, ṙ) phase curves are more complicated. Also, resorting to the (rθ̇, ṙ)-plane of the polar components of velocity, the trajectories are found again to be conic sections (Mioc & Stoica 1995c), but the rectilinear motion cannot be studied in such a way.

4. Physical interpretation

Let us first clear up the nature of the physical motion represented geometrically in figures 1-3. By (4), u varies monotonically (if $C \neq 0$) or remains constant (if $C = 0$) all along the motion. Consequently, every segment of trajectory in the upper/lower halfplane of figures (where 1/r increases/decreases monotonically) physically means spiral ($C \neq 0$) or radial ($C = 0$) motion performed outwards/inwards. This is valid only for figure 1; the physical motion corresponding to figures 2 and 3 cannot be rectilinear because $\delta \geq 0$ implies $C \neq 0$, hence radial motion is not possible.

Now, let us interpret the figures in terms of physical motion. Consider that $C^2 < 3(\mu/c)^2$ (figure 1). If $h < 0$ the orbits eject from collision, reach a maximum distance $r_{max} = \mu/[\r(h_c(h_c - h)) - h_c]$ (easily obtainable from the quantitative characteristics given in Section 3), and then tend back to collision (no escape is possible). If $h \geq 0$ the orbits either eject from collision and tend to infinity, or come from infinity and tend to collision.

If $C^2 = 3(\mu/c)^2$ (figure 2) the scenarios are qualitatively the same as in the previous case. However, radial motion is not possible, and $r_{max} = -2\mu/h$ for $h < 0$.

Finally, let $C^2 > -3(\mu/c)^2$ (figure 3). If $h = h_c$ (< 0) we have stable equilibrium circular orbits of radius $r_e = -\mu/h_c$. If $h_c < h < 0$ the motion has periodic character (neither collision nor escape are possible). The real, physical orbits are precessional ellipses lying inside an annulus defined by $r_{min} = \mu/[\sqrt{h_c(h_c - h)} - h_c]$ and $r_{max} = -\mu/[\sqrt{h_c(h_c - h)} + h_c]$. The motion is periodic (closed curves, rosette-shaped) or quasiperiodic (unclosed rosettes filling densely the annulus). Expressions (7) show that most of such orbits are quasiperiodic (the set of periodic solutions having measure zero). If $h \geq 0$ the orbits come from infinity, reach a minimum distance $r_{min} = \mu/[\sqrt{h_c(h_c - h)} - h_c]$, and then tend back to infinity (no collision is possible).

To have a more detailed picture of the physical motion, if $C = 0$ the collision (ejection is rectilinear. If $C \neq 0$ the situation changes: the particle (m_2) spirals performing infinitely many loops around the centre (m_1) immediately before collision (after ejection). This is the so-called black hole effect, whose occurrence makes the set of initial conditions leading to collision (ejection) have positive measure (Diacu *et al.* 1995).

At collision (ejection) the velocity has an infinite value. As to the asymptotic velocity at infinity, its value is zero for $h = 0$ and positive ($\sqrt{h}$) for $h > 0$.

These results offer a wide picture of the two-body problem in Maneff's field from a twofold standpoint: geometrical and physical.

5. Astronomical implications

Our qualitative analysis was performed from the standpoint of the (abstract) celestial mechanics. Let us now look briefly at these results from an astronomical perspective.

Observe that the second term in (1) can be regarded as being a perturbing function in a Newtonian two-body problem. As the "perturbing force" is central, recall that the focal parameter of the osculating conic sections remains constant all along the motion ($p = p_0$). Suppose that $C^2 (= \mu p_0) \leq 3 (\mu/c)^2$; this leads to $p_0 \leq 3\mu/c^2 = (3/2)R_{Sch}$ (where $R_{Sch} = 2\mu/c^2$ is the Schwarzchild radius of the central body). In other words, in such cases the (global) trajectories will necessarily be of the type collision-collision, ejection-escape, or infinity-collision, as our qualitative results showed (figures 1 and 2).

Consider now the most interesting case, $C^2 > 3(\mu/c)^2$, in which, *for point masses*, the motion is noncollisional. However, for concrete celestial bodies, of finite dimensions, the situation changes a little. To exemplify, choose a typical pulsar of 1.4 solar masses and radius $R = 15$ km, and a test particle moving under its gravitational action. With these values, the condition for C^2 reads $C^2 > 1.15 \times 10^{12}$ km^{4}s^{-2}, but this is an idealization. To be sure that the motion is noncollisional ($r_{min} > R$), we must consider $C^2 > 2.8 \times 10^{12}$ km^{4}s^{-2} for $h = h_c$, while for other energy levels the following relation (easily obtainable from the formulae given in Sections 3 and 4) must be fulfilled: $h < C^2/225 - 5.3 \times 10^{12}$ (with h expressed in km^{2}s^{-2} and C^2 in km^{4}s^{-2}). Under these conditions, the scenarios presented in Section 4 are recovered.

To end this section, let us consider the evolution of a very well known astronomical two-body system in Maneff's field: the binary pulsar PSR 1913+16. This system is acting very close to the ideal of two point masses. On the basis of the characteristics given by Lyne & Graham-Smith (1990), we found $C^2 = 2.1 \times 10^{17}$ km^{4}s^{-2}, $3(\mu/c)^2 = 4.6 \times 10^{12}$km^{4}s^{-2}, $h < 0$, hence the trajectory is a precessional ellipse. By (7c) it is easy to determine that, for an orbital period of 27907 seconds, the rate of periastron advance is of order 4.3 degrees yearly, in agreement with the measured value.

6. Conclusions

Compared with the Keplerian trajectories in the Newtonian two-body problem, those corresponding to Maneff's field present the following main particularities: (1) they are not fixed, but precessional conic sections; (2) collisions occur not only for radial motion ($C = 0$), but also for curvilinear trajectories with $C^2 \leq 3(\mu/c)^2$; (3) while in Newton's field the collisional rectilinear motion is the limit case of more and more eccentric ellipses, this is not true in Maneff's field (see Diacu *et al.* 1995); (4) in both models there exists the equilibrium solution of circular motion. Of course, in concrete astronomical situations, specific conditions (e.g. $r_{min} > R$ for noncollisional orbits) must be observed for both fields.

As regards a comparison with the relativity theory, Maneff's model provides the same periastron advance, verified both qualitatively and quantitatively. Other effects predicted by the relativity are also recoverable within this framework (see Maneff 1925).

Maneff's gravitational model is worth studying for several reasons concerning mainly celestial mechanics and astronomy. It maintains the simplicity and the advantages of the Newtonian model, and also provides the necessary corrections such that orbits coming close to collisions match theory with observations. Within its framework the natural, unperturbed motion of a celestial body is precessional, as relativity foresaw. In such a field, due to the particularity (2) above, the set of initial data leading to collisions has positive measure (and in the solar system the collisions are not so rare as the Newtonian model asserts). A supplementary argument: the *black hole effect*, considered in astrophysics (see Lyne & Graham-Smith 1990; Stephens 1996), is possible in Maneff's field, as well as in relativistic fields, but not in Newton's one.

As a final conclusion, to better understand (both quantitatively and qualitatively) many astronomical situations, the powerful tool of relativity is not strictly necessary. Its predictions are recoverable in the framework of classical mechanics by resorting to Maneff's model, much more suitable for the theoretical needs of celestial mechanics.

Acknowledgement

Useful comments and suggestions of the anonymous referee are duly acknowledged.

References

Delgado J., Diacu F.N., Lacomba E.A., Mingarelli A., Mioc V., Perez E., Stoica C., 1996, J. Math. Phys., 37 (in press).

Diacu F.N., 1993, J. Math. Phys., 34, 5671.

Diacu F.N., 1996, J. Diff. Eq. (in press).

Diacu F.N., Mingarelli A., Mioc V., Stoica C., 1995, in Dynamical Systems and Applications, ed. R.P. Agarwal, WSSIAA, Vol. 4, World Scientific, Singapore, p. 213.

Hagihara Y., 1975, Celestial Mechanics, Vol. 2, Part 1, MIT Press, Cambridge, Massachusetts.

Lacomba E.A., Llibre J., Nunes A., 1991, in The Geometry of Hamiltonian Systems, ed. T. Ratiu, Springer-Verlag, New York.

Lyne A.G., Graham-Smith F., 1990, Pulsar Astronomy, Cambridge Univ. Press, Cambridge.

Maneff G., 1924, C.R. Acad, Sci. Paris, 178, 2159.

Maneff G., 1925, Z. Phys., 31, 786.

Maneff G., 1930a, C.R. Acad, Sci. Paris, 190, 963.

Maneff G., 1930b, C.R. Acad, Sci. Paris, 190, 1374.

Mioc V., Stoica C., 1995a, C.R. Acad, Sci. Paris, ser.I, 320, 645.

Mioc V., Stoica C., 1995b, C.R. Acad, Sci. Paris, ser.I, 321, 961.

Mioc V., Stoica C., 1995c, Bull. Astron, Belgrade, No.152, 43.

Stephens S., 1996, Astronomy, 24, 50.